








Understanding the European energy crisis through structural causal models

Anton Tausendfreund ^{1,2,*} Sarah Schreyer ^{1,2,*} Florian Immig ^{3,*} Ulrich Oberhofer ³
Julius Trebbien ^{1,2} Aaron Praktijnjo^{4,5} Benjamin Schäfer ³ and Dirk Witthaut ^{1,2,5,†}

¹*Institute of Climate and Energy Systems: Energy Systems Engineering (ICE-1),
Forschungszentrum Jülich, 52428 Jülich, Germany*

²*Institute for Theoretical Physics, University of Cologne, 50937 Köln, Germany*

³*Institute for Automation and Applied Informatics,*

Karlsruhe Institute of Technology, 76344 Eggenstein-Leopoldshafen, Germany

⁴*Chair for Energy System Economics, Institute for Future Energy Consumer Needs and Behavior (FCN),
E.ON Energy Research Center, RWTH Aachen University, 52074 Aachen, Germany*

⁵*JARA-ENERGY, 52074 Aachen, Germany*

Natural gas supplies in Europe were disrupted and energy prices soared in the context of Russia's invasion of Ukraine. Electricity prices in France experienced the largest relative increase among European countries, even though natural gas plays a negligible role in the French electricity system. In this article, we demonstrate the importance of causal statistical methods and propose causal graphs to investigate the French electricity market and pinpoint key influencing factors on electricity prices and net exports. We demonstrate that a causal approach resolves paradoxical results of simple correlation studies and enables a quantitative analysis of indirect causal effects. We introduce a linear structural causal model as well as non-linear tree-based machine learning combined with Shapley flows. The models elucidate the interplay of gas prices and the unavailability of nuclear power plants during the energy crisis: The high unavailability made France dependent on imports and linked prices to neighboring countries.

INTRODUCTION

The European energy system is dependent on imports of natural gas and other fossil fuels [1, 2]. Natural gas supplies were disrupted in the context of the Russian invasion of Ukraine, as major pipelines pass through Ukraine, and Russia shut down the NordStream1 pipeline in July 2022 [3]. Market prices for natural gas and electricity spiked across Europe, with gas prices peaking at 330 EUR/MWh (Fig. 1a). As a result, energy prices and energy security have become dominant issues in the political debate across Europe [4]. Many countries have lowered energy taxes [5] and increased efforts to reduce consumption [6]. The European Union adopted measures to reduce import dependency from Russia and promote the security of supply [7, 8].

Notably, electricity markets were affected quite differently during the crisis [9]: The relative price increase was lowest in Poland and the Northern parts of Norway, while strong effects of the relative price were observed in Norway's southernmost bidding zone NO2 and in France. In both regions electricity market prices increased by almost a factor of four (Fig. 1b). This is very surprising as natural gas plays a negligible role in electricity generation in both countries. France relies mainly on nuclear power and Norway mainly on hydroelectric power [10]. So what caused the drastic increase in electricity prices? Why were France and Norway affected so strongly while they do not rely on gas?

The political debate about energy prices and the design of the future energy system remains highly controversial, particularly with regard to the role of nuclear power

plants [13, 14] and renewable energy sources (mainly hydro, wind and solar) [15, 16]. Empirical research on electricity prices and their drivers is needed to enable informed decisions. With the increasing amount of available data [10], data-driven approaches become feasible and potentially necessary [17, 18] to handle the enormous amount of available information. Critically, such analysis should not be limited to black-box predictions or correlation analysis but needs to inform interventions. Hence, causal explanations are required [19].

In this article, we show the importance of a *causal* analysis of electricity market data in the context of the European energy crisis. We present two approaches based on causal graphs: linear structural causal models [20] and non-linear tree-based machine learning combined with Shapley flows [21]. We focus on the French electricity market and disentangle the role of rising natural gas prices and problems with the nuclear fleet, which occurred coincidentally. Furthermore, we analyze indirect causal effects and quantify how weather effects, such as river flow and temperature, affected load and nuclear availability and thereby prices and export capacities in France. Although the onset of the energy crisis spans a period of time, we fix October 1, 2021, as a reference date for clarity and compare the periods before and after.

RESULTS

Correlation and causality in electricity markets

The French electricity system is mainly based on nuclear power. In 2022 and 2023, several plants were out of

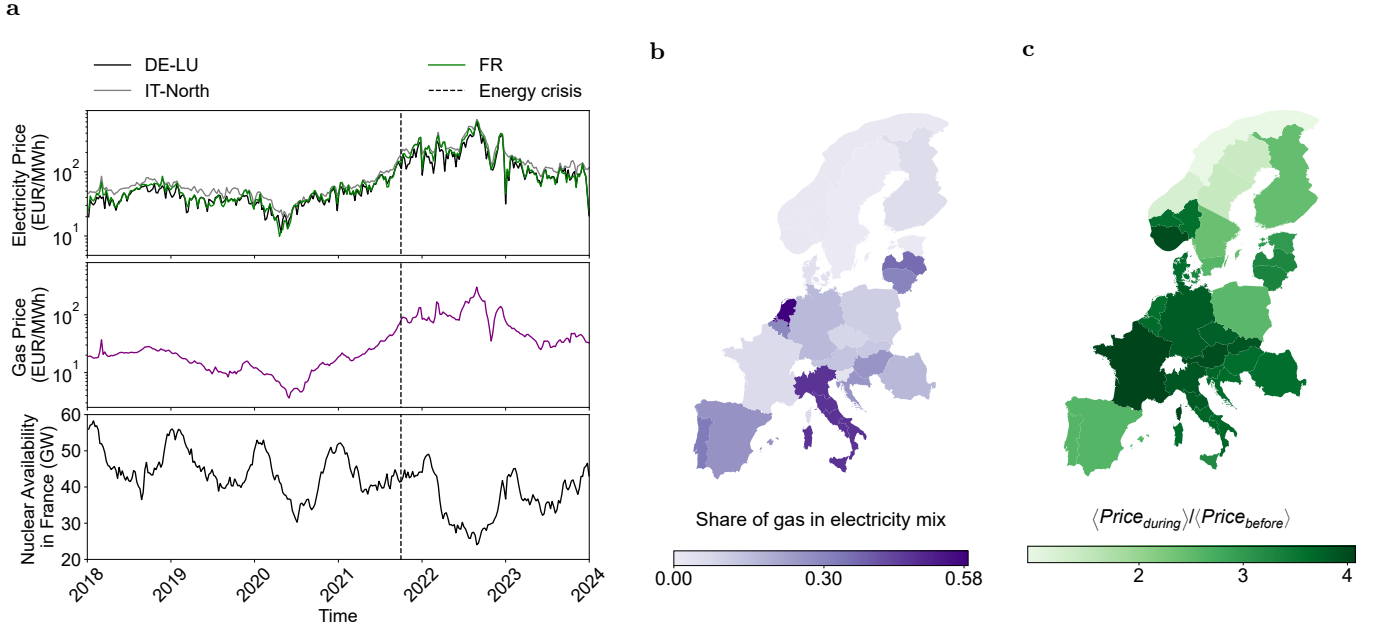


FIG. 1. **The European energy crisis.** **a**, Energy prices soared in connection to the Russian invasion of Ukraine. Here, we show gas prices from the Dutch TTF daily future market and electricity prices from the day-ahead spot markets in the bidding zones France (FR), Germany-Luxembourg (DE-LU) and Italy North (IT-North) averaged weekly on a logarithmic scale. In France, the available nuclear power dropped to very low values during the crisis due to urgent revisions. Prices increased well before the invasion; here we identify October 1st (dashed line) as the begin of the energy crisis. **b**, The share of natural gas in the electricity mix differs strongly between European countries. Data was taken from before the crisis from the year 2020. **c**, Relative increase of electricity market prices in the different bidding zones. Prices in France and Southern Norway increased by a factor of approximately four, although the contribution of natural gas is negligible in these countries. Raw data has been obtained from Thomson Reuters [11], ENTSO-E [10] and Eurostat [12] (see Methods for Details).

operation due to delayed maintenance, corrosion problems or lack of cooling water [22]. As a result, nuclear availability reached historically low levels during the energy crisis. Approximately half of the nuclear power plants were not available in summer 2022, and the availability occasionally dropped below 30 GW (Fig. 1a). It is therefore plausible that problems with the nuclear fleet were a major contributor to rising electricity prices. These problems were specific to the French electricity system and may explain why France was more affected than neighboring countries.

However, empirical validation of this hypothesis is not straightforward. A naive data analysis shows that the correlation between electricity prices and nuclear availability is positive (Fig. 2b). That is, the price appears to increase with the availability of nuclear power and thus with higher supply, in clear violation of economic laws. To resolve this paradox, we need to distinguish causal effects from mere correlations. The French electricity system is subject to strong seasonal effects that lead to confounding: The load, and thus the demand, is significantly higher in the winter than in the summer and high prices typically occur in winter (see Supplementary Information). Hence, revisions take place mostly in the summer where both demand and electricity prices are lowest and thus the opportunity costs for unavailability

are lowest. Thus, the observed positive correlation between price and nuclear availability does not necessarily indicate a causal effect.

This situation is illustrated in Fig. 2a, where arrows indicate potential causal effects between two variables. The correlations between prices and nuclear availability are determined by two paths: the direct causal link and an indirect path via the time of the year and the load. The indirect path leads to for confounding: The time of year affects both nuclear availability (through outage planning) and load, which then affects price. This indirect path is not causal; in the graph we have to pass an arrow against its causal direction to get from nuclear availability to price. Nevertheless, the indirect path essentially determines the correlations.

To estimate the causal effect of nuclear availability on prices, we need to break the spurious path by fixing one of the variables. We do this by dividing the data set according to different values of the load L . For each chunk of data, we observe a negative correlation between electricity prices and nuclear availability (Fig. 2b). In other words, the paradox is resolved and the economic laws of supply and demand hold as expected.

A similar behaviour is observed for French net exports, i.e. the difference of all exports and imports per hour. The raw data shows a negative correlation to the

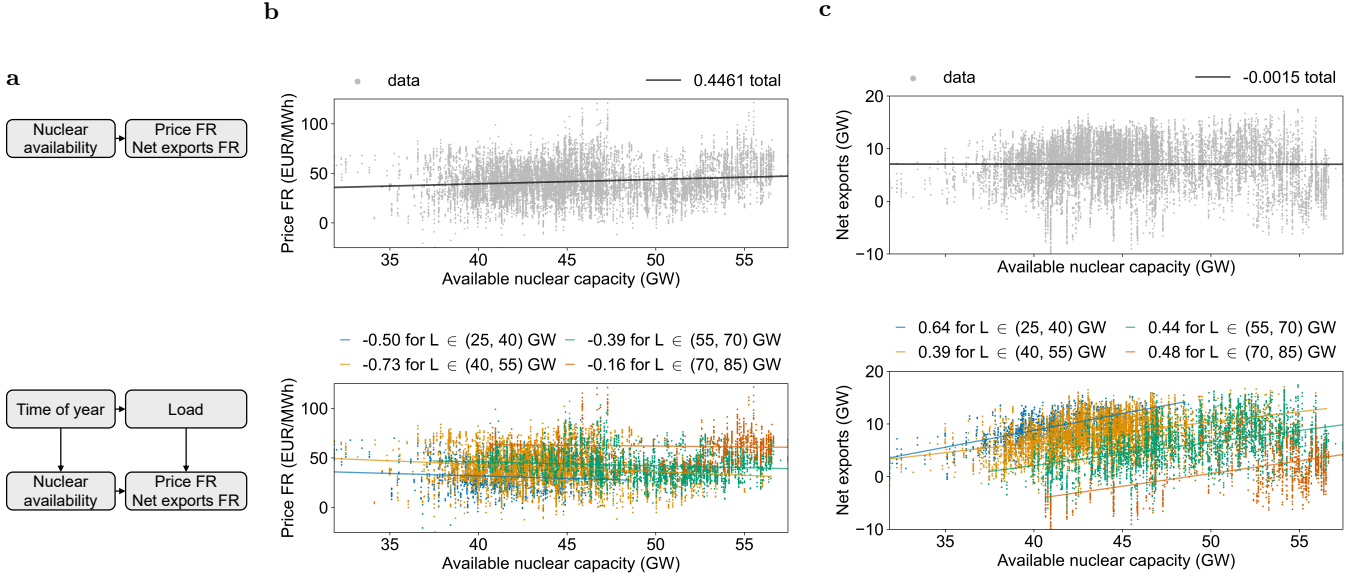


FIG. 2. **Simpson's paradox in the French electricity market.** **a**, Graphical representation of the relation of the available nuclear capacity and the electricity price, where causal effects are represented by arrows. In the top row we ignore confounding effects. In the bottom row we include confounding due to seasonality and load. **b**, Relation of the available nuclear capacity and the electricity price. The price seemingly increases with the capacity, in clear violation of economic laws (upper panel). This is an example of Simpson's paradox, where a statistical correlation is observed when the entire data is considered, but reverses for subsets of the data [20]. The paradox is resolved if we adjust for confounding, by splitting the time series in four chunks according to the load L (lower panel, indicated by different colors). The slope of a linear fit is negative for all chunks. The slopes are given above the panel in units of $\text{EUR MWh}^{-1} \text{GW}^{-1}$. **c**, A similar pattern is observed for the net exports, i.e. the difference of electricity exports and imports. A linear fit to the entire dataset yields a negative slope contrary to expectations. Splitting the data to four chunks according to the load L yields a positive slope as expected. The dimensionless slopes are given above the panel. Here, we use data from 2018-04-01 to 2020-04-01 only to exclude impacts of the energy crisis and better show the Simpson's paradox. Every data point corresponds to one hour.

available nuclear capacity. After fixing the confounding factor, we observe, as expected, a positive correlation (Fig. 2c).

The above example shows that advanced statistical methods are needed in the empirical analysis of electricity markets. In particular, we need methods of *causal* inference to deal with confounders and to distinguish correlations from causal effects. In what follows, we turn to structural causal models for quantitative analysis.

A structural causal model for electricity prices

We propose a structural causal model (SCM) to analyse the French electricity market during the energy crisis (Fig. 3). The starting point is the formulation of a causal graph, where each variable of interest X_i is described by a node or vertex [20]. A potential causal interaction of two variables is described by a directed edge.

The electricity price and net export are mainly affected by load, renewable generation, availability of other plants, and prices for natural gas and carbon emissions [23, 24]. To capture the effects of cross-border trade, we include the residual load, i.e. the difference

between load and renewable generation, for all neighboring bidding zones. We note that Switzerland and the UK are excluded as they are not part of the single day-ahead coupling mechanism [25]. Finally, we include the residual load ramp to capture possible effects of ramping constraints [24, 26]. The feature variables themselves depend on calendrical and meteorological variables.

In an SCM, each variable X_i is described by a structural equation $X_i := f_i(PA_i, U_i)$, where PA_i is the set of parents of X_i in the causal graph and U_i describes unobserved variables. Restricting ourselves to linear equations enables a straightforward interpretation of the results. The structural equations simplify to

$$X_i := \sum_{j \in \text{parents}(i)} c_{ij} X_j + U_i, \quad (1)$$

where the structural coefficient c_{ij} describe the direct causal effect of the variable X_j on the variable X_i . We emphasize that although we use regression to infer structural coefficients, these coefficients are *not* identical to ordinary regression coefficients. Structural coefficients assume causation, regression coefficients do not [20].

Fitting a linear SCM to the French data yields the structural coefficients shown in Fig. 4. Further results

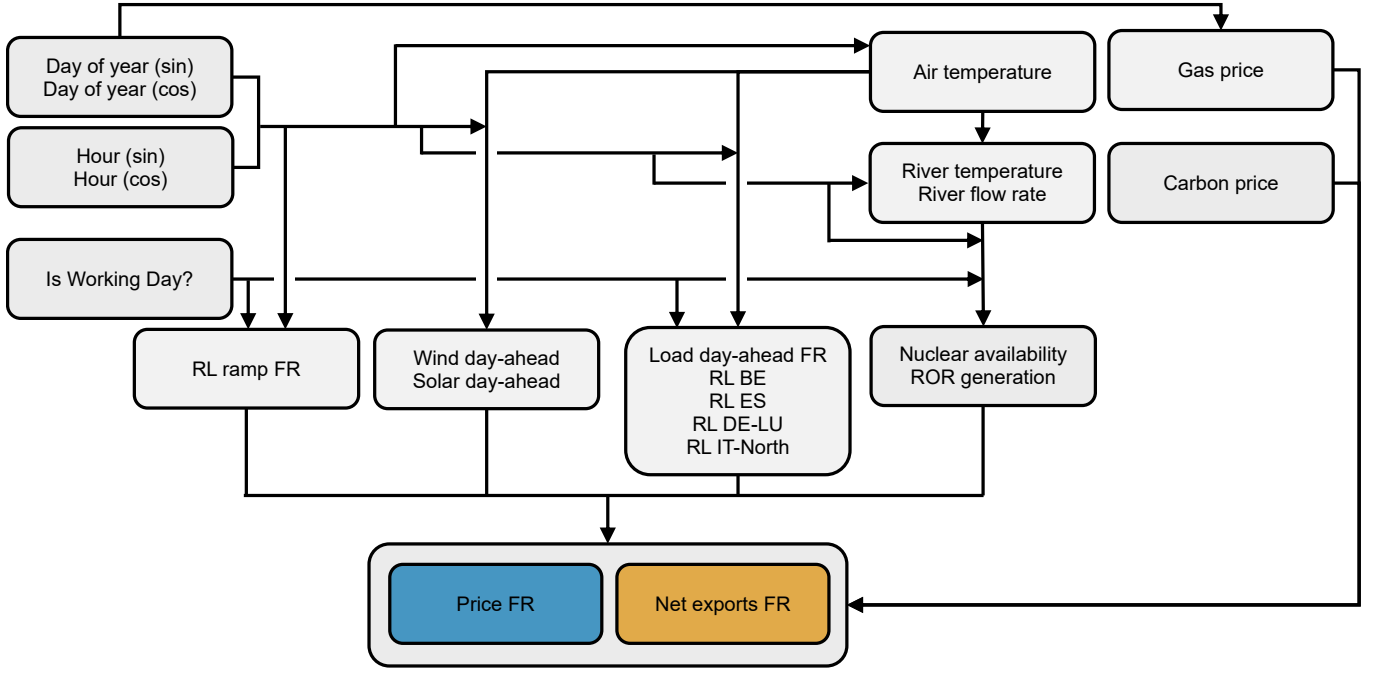


FIG. 3. **Structural causal model (SCM) for the French electricity market.** We propose a causal graph for the analysis of electricity prices and net exports. Boxes represent calendrical, meteorological and energy system variables included in our analysis (see main text for details). Variables with the same neighbors in the causal graph are grouped for the sake of clarity. Arrows indicate potential causal interactions between variables. We use the abbreviations ROR for run-of-river hydro power and RL for the residual load, i.e. load minus must-run capacity.

and an evaluation of the model can be found in the supplementary information. To capture the role of each variable during the energy crisis, we also plot the quantity

$$c_{ij}\Delta\bar{X}_j = c_{ij} \left(\langle X_j \rangle_{\text{during}} - \langle X_j \rangle_{\text{before}} \right), \quad (2)$$

where $\langle X_j \rangle_{\text{before/during}}$ denotes the average of the respective variable before and during the crisis. This variable quantifies how a change in the variable X_j during the energy crisis causally affected the variable X_i on average.

We find that the natural gas price is the most important variable affecting the electricity market price in France. The availability of nuclear power comes second, but to a much lesser extent. The importance of the gas price is not generally unexpected: In many electricity markets, gas-fired power plants are the last to enter the market according to the merit order principle [27]. Their bids therefore determine the market clearing price. However, the result is surprising in this context as natural gas plays a minor role in the French electricity market (Fig. 1b). In particular, it does not explain why France was hit so hard during the energy crisis.

France has been a net exporter of electricity for decades. With large parts of its nuclear fleet under revision, France could no longer maintain these exports and became a net importer in 2022 [9]. The crucial role of nuclear availability for cross-border trading is confirmed by our structural causal model (Fig. 4d). We find that

the difference in nuclear availability before and during the crisis essentially determines the sharp fall in France's net exports.

Cross-border trade is closely linked to price differences. The European market coupling algorithm EUPHEMIA will generally increase exports to neighbouring countries when prices are lower and transmission capacity is available [9, 28]. The sharp fall in French net exports is thus associated with a reversal of price differences with respect to Germany, Belgium and Spain (see Supplementary Information).

We conclude that the interplay of two factors caused the sharp rise in French electricity prices [22]. The massive unavailability of nuclear power plants made France dependent on its neighbors and tied prices together. Rising gas prices propagated to the electricity markets in Italy, Germany and Belgium and eventually affected prices in France.

It must be emphasized that the situation in the French electricity system could have been much more severe without the option to compensate lacking domestic generation by imports. European cooperation contributed to France's security of supply, but also to its electricity prices.

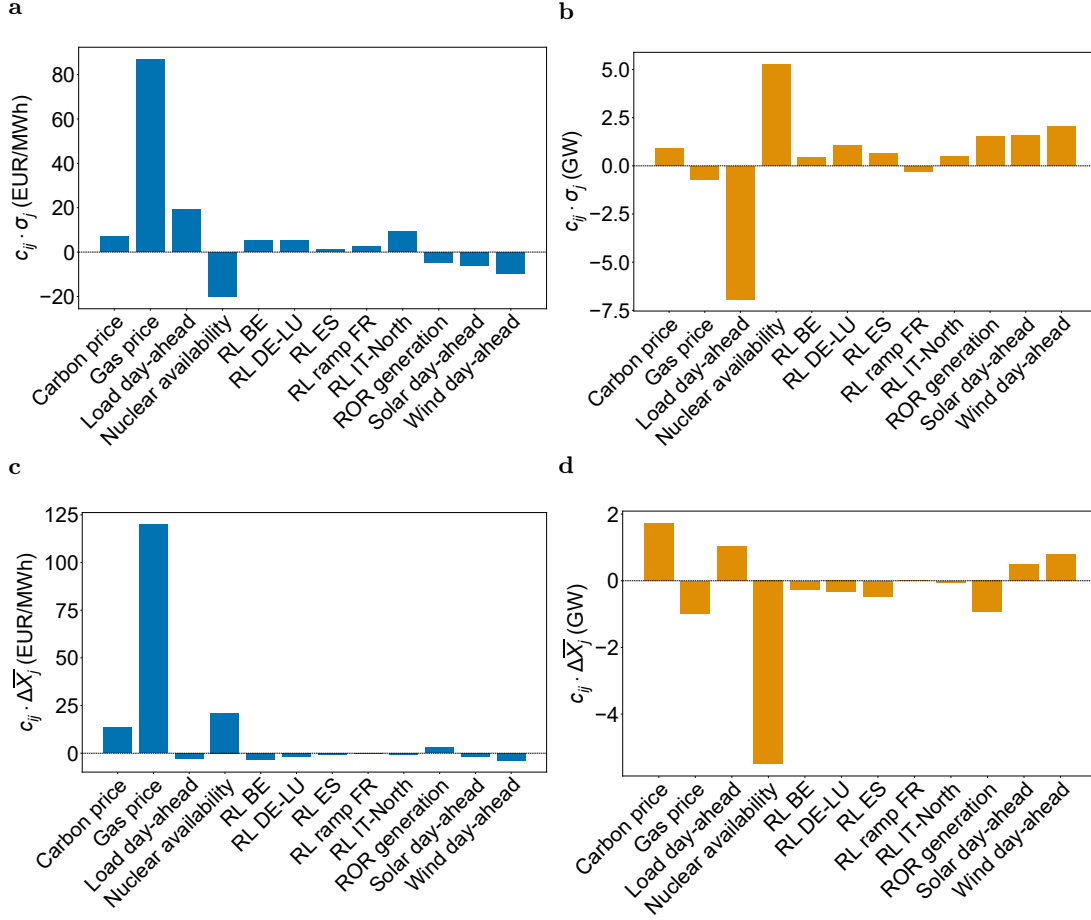


FIG. 4. **Results of the SCMs for the French electricity market.** Results are shown for **a,c** the electricity market prices and **b,d** the net exports. **a,b** Structural coefficients c_{ij} of the SCM normalized by the standard deviation σ_j of the predictor variable to enable comparability. **c,d**, Structural coefficients c_{ij} multiplied by the average difference of the variable before and during the energy crisis $\Delta \bar{X}_j$ as defined in Eq. (2). This quantity measures the impact of changes in the predictor variable on the respective target. For the day-ahead price, the increase of the gas price has the strongest impact with more than +120 EUR/MWh. For the net exports, the decrease of the nuclear availability had the strongest impact with -5.5 GW.

Indirect causal effects: Hydropower and cooling water

Structural causal models can consistently quantify indirect causal effects. We examine the role of rivers, which provide cooling water for most nuclear power plants, as well as run-of-river hydropower. In recent years, French power plants have repeatedly experienced operating restrictions due to lack of cooling water during hot and dry summers [29]. Climate models predict that precipitation and river flows in France will decrease significantly under scenarios of continued high greenhouse gas emissions [30]. Model-based studies have quantified the potential impact on thermoelectric and hydropower generation [31, 32]. Here we provide an empirical analysis of the impact of river flows on electricity prices.

In our SCM, we have aggregated the time series of river flows of several French rivers into one variable for simplicity (see Methods for details). This variable en-

ters the models of nuclear availability and run-of-river hydropower (Fig. 3), both of which affect the electricity price. In a linear SCM, the indirect causal effect is obtained by simply multiplying the structural coefficients [20]. Summarising both causal paths, we find that a decrease in flow of $1 \text{ m}^3/\text{s}$ increases electricity prices by 0.056 EUR/MWh on average (Fig. 5). Interestingly, both causal pathways contribute to a similar extent.

Again, a naive data analysis does not properly account for the effect of river flows. A direct linear regression on the raw data yields a slope of $-0.176 \text{ EUR/MWh} \cdot \text{s/m}^3$ and overestimates the causal effect by a factor of approximately three. This overestimation is a consequence of confounding due to seasonality effects. Typically, river flow rates are highest in winter and spring when electricity prices are high and smallest in summer when prices are low. Thus seasonality introduces an anti-correlation between the river flow rate and the price.

A similar analysis of the indirect impact of the river

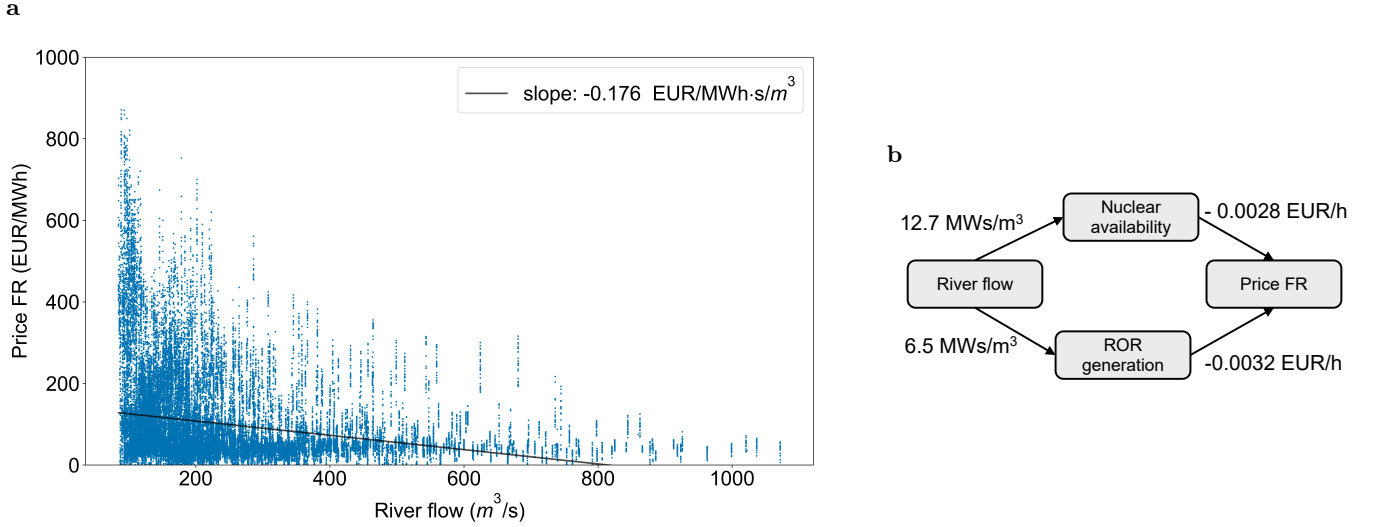


FIG. 5. **Indirect impact of river flow on electricity price.** **a**, Scatter plot of the electricity price against the river flow rate. A linear regression yields a slope of $-0.176 \text{ EUR/MWh} \cdot \text{s/m}^3$. **b**, Extract of the causal graph showing the indirect impact of river flow on electricity price through nuclear availability and run-of-river hydro (ROR) generation. The arrows indicating causal relations are labeled with the respective structural coefficients. The indirect causal effect is calculated by multiplying the structural coefficients of each causal path and summarizing both paths. This leads to an indirect causal effect $-0.056 \text{ EUR/MWh} \cdot \text{s/m}^3$, significantly less than the regression coefficient. The discrepancy can be explained by confounding due to seasonality effects.

flow on the net exports is provided in the supplementary information.

Shapley flows

Linear SCMs are inherently transparent but they cannot account for non-linear relationships in the data. Therefore, we complement our analysis with a Gradient Boosted Tree (GBT) model, which can account for arbitrary relationships. While GBTs are not inherently transparent, we still obtain efficient ex-post explanations of the model using Shapley additive explanations (SHAP) [33]. Since standard SHAP values do not include causal knowledge, we utilize the Shapley flows extension [21], which explains the model in terms of a causal graph (see Methods).

Combining a causal graph with a GBT model provides further insights into the causal flow (Fig. 6). In this case, the GBT model predicts the net export from France given the external features; results for electricity prices are provided in the Supplementary Information. Interpreting from right (target and leaf of the causal graph) to left (roots of the causal graph), we initially note how the Nuclear availability and Load day-ahead features have the largest direct impact on the target. This is consistent with our domain understanding and the linear SCMs (Fig. 4): high loads and low nuclear availability lead to lower exports, as the domestic demand is fulfilled first. Moving to the left, we note how the load itself is heavily influenced by calendrical features and the temperature

feature. Electric heating plays a major role in France contributing to a temperature-dependence of the load [34]. The other directly relevant feature, the availability of nuclear power plants, is mostly affected by the day of the year and the river flow rate, which in turn is mostly affected by the temperature. Again, this is consistent with our domain understanding: High temperatures cause (or at least coincide with) low levels of river flow, which in turn limit the capability of thermal power plants to cool and hence generate electricity.

Shapley flows explain the nonlinear dependencies learned by the model and allow to disentangle direct and indirect effects as shown Fig. 7. Based on the insights of Fig. 6, we specifically follow the flows from Air temperature and River flow rate via selected intermediate features towards the net export target. Note that also the indirect effects are still measured towards the target variable. The effect of Air temperature on the net exports via the load day-ahead feature is initially almost linear (Fig. 7 a) before saturating around 10°C . This aligns with our intuition: for large enough temperatures, heating does not play a major role in the load and hence does not affect exports substantially. This interpretation is further supported when analyzing the direct contribution of load day-ahead values on net exports (Fig. 7 b): The two entities follow an almost perfect linear relationship with negative correlation, i.e. lower load values allow higher exports. In contrast, the impact of river flow rate on the net exports via the nuclear availability is more complex (Fig. 7 c): For very low flow rates, the nuclear availability drops and hence the exports decrease. Mean-

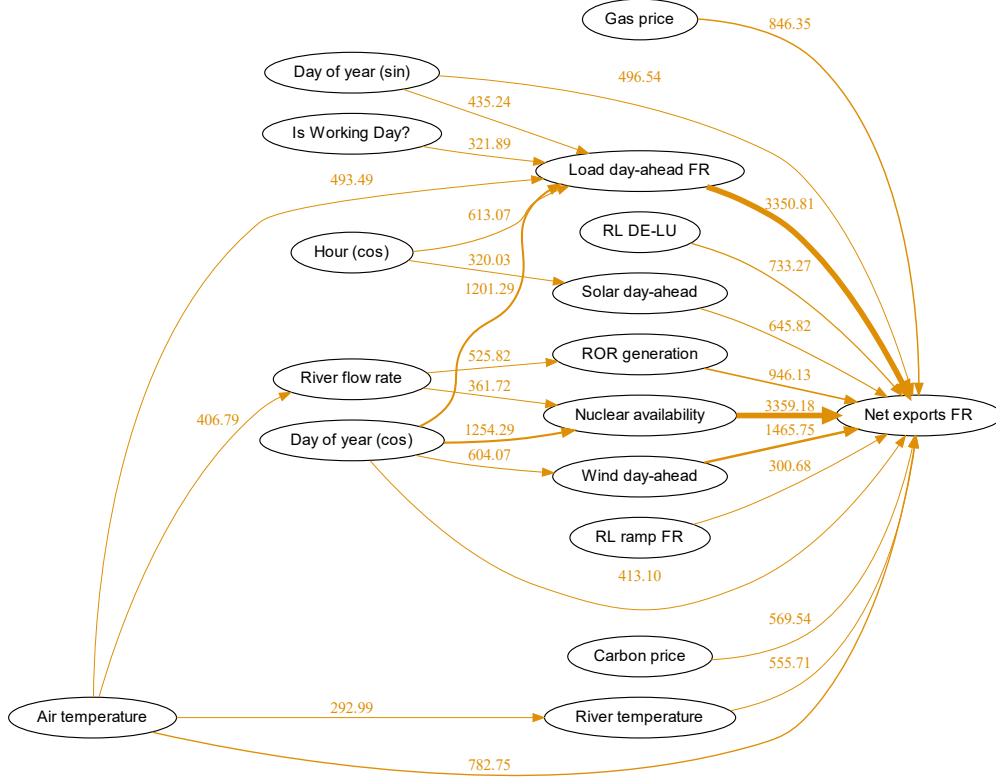


FIG. 6. **Shapley flows explain the non-linear GBT model for the net exports.** All feature and the target node of the causal graph are shown. In contrast to the causal graph shown in Fig. 3, only the 25 most important edges are shown. The edge attributions quantify how a given feature directly or indirectly influences the target prediction. For example, the Air temperature feature has both relevant direct and indirect effects across the graph.

while, for larger flow rates, a more complex dependency is learnt with several interacting features, leading to the observed scattering. The effect of the flow rate via ROR generation is smoother (Fig. 7 e) but again lower flow rates cause lower ROR generation and hence lower exports. The direct impact of both nuclear availability (Fig. 7 d) and ROR generation (Fig. 7 f) is both approximately linear with a positive correlation. As was already visible in Fig. 6, the effect of nuclear availability is about thrice that of ROR generation.

Summarizing, GBT models with Shapley flows provide more detailed insights and consistency checks. We find that the relations of the target and its parents in the causal graph are mostly linear, confirming the insights from the linear SCM. In contrast, Shapley flows reveal strongly nonlinear indirect effects, as demonstrated for the temperature and the river flow rate. Notably, this analysis is not possible with linear SCMs or ordinary SHAP values [21].

DISCUSSION

Transparency and empirical verification are essential in energy systems research [35]. In this article we have demonstrated the importance and perspectives of causal statistical models in energy systems analysis. Simpson’s Paradox (Fig. 2) shows that simple correlation studies can be highly misleading and thus inadequate for empirical studies. Causal graphs resolve this paradox and pave the way for causal machine learning models. We have applied such models to the French electricity market, which was severely affected during the European energy crisis.

We emphasize that both models of French electricity prices and net exports have high R2 scores for the respective final targets but mediocre scores for intermediate variables (see Supplementary Information). Nuclear availability for example has a R2 score of 44 % since important influencing factors are not considered. For example, in 2021 and 2022 an unforeseen stress corrosion phenomenon lead to many reactors going into revision [36]. We remark that this is not crucial in the current setting because we mainly focus on the results for elec-

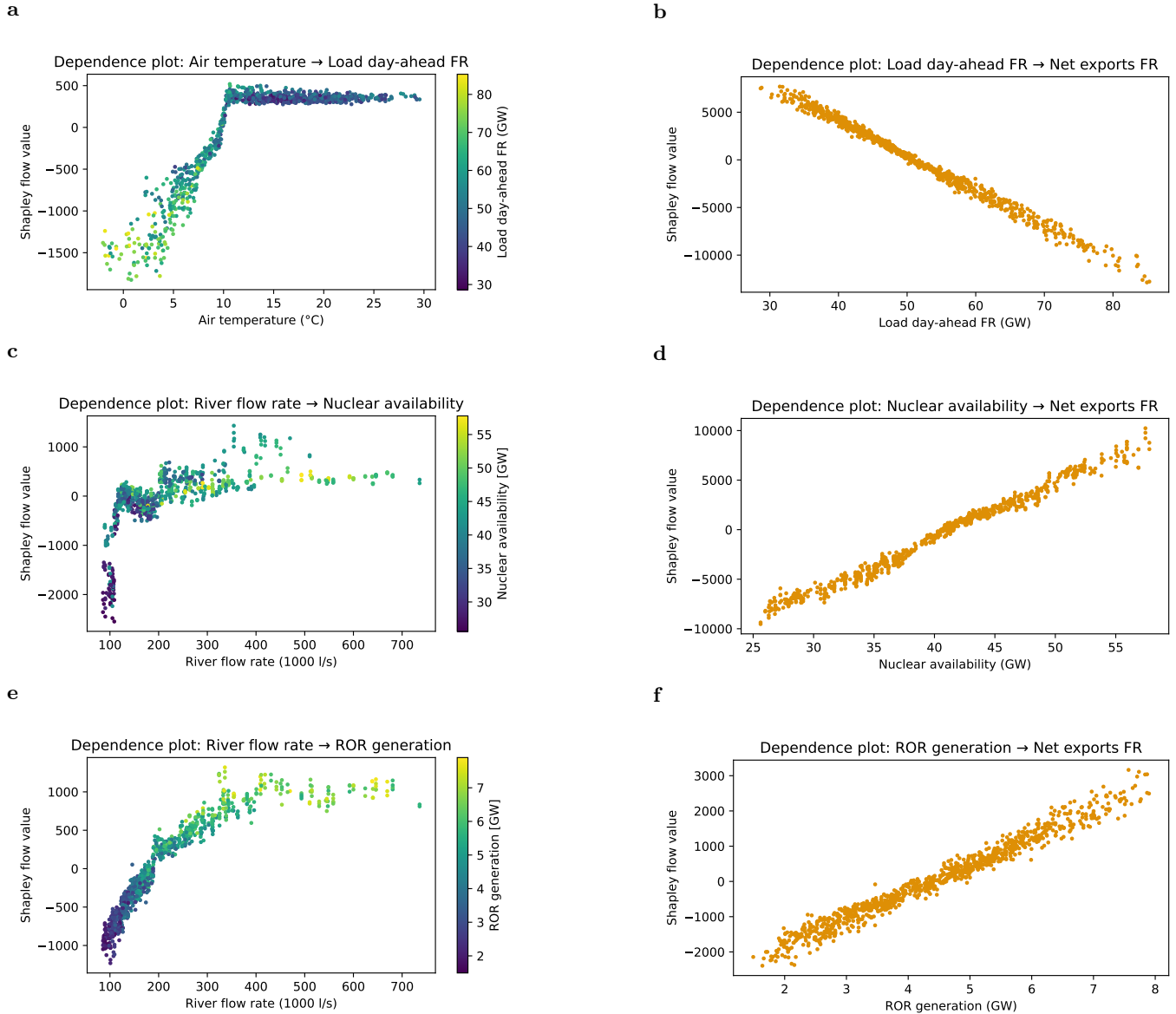


FIG. 7. Shapley flow analysis reveal direct linear and indirect non-linear dependencies. We display Shapley flow dependencies plots for the target of net exports. We follow the causal flow from Air temperature via day-ahead load (a) to the target (b). Similarly, we visualize how river flow rate impacts nuclear availability (c) and ROR generation (e) which both directly impact the target (d,f)

tricity price and net exports.

We argue that two main factors caused the sharp rise in electricity prices in France: the low availability of nuclear power plants and the soaring price of natural gas. With up to half of its nuclear fleet under revision, France's electricity imports increased sharply and electricity market prices in France and its neighbouring countries often synchronised. As the overall level of electricity prices rose during the European energy crisis, so did the level of prices in France.

We hypothesise that the price increase in Norway's southernmost bidding zone NO2 was also caused by two factors. The NordLink interconnector between Ger-

many and Norway and the North Sea Link interconnector between the UK and Norway were commissioned in 2021, just before the start of the European energy crisis. With a capacity of 2×1.4 GW, imports and exports via these interconnectors can significantly affect the electricity market in southern Norway. Electricity prices can be synchronised with those in Germany or the UK, where natural gas plays an important role in the electricity system. Future work will investigate this further.

Beyond our contributions understanding the effects of the energy crisis, we further advocate the usage of structural causal models and causal explanations of machine learning models: These tools provide causal insights into

complex problems, as we often encounter them in the energy system.

METHODS

Data sources and pre-processing

Time series data on installed nuclear capacity, unavailable nuclear capacity, day-ahead wind generation, day-ahead solar generation, day-ahead load, actual run-of-river and poundage (ROR) generation, scheduled commercial exchange and day-ahead electricity price were obtained from the ENTSO-E transparency platform [10]. The data was retrieved using the ENTSO-E restful API using the open source python package `entsoe-py` [37]. We include the residual load of neighboring countries who participate in the Single Day-Ahead Coupling (SDAC) of electricity markets throughout the period of our study [38]. Multiple bidding zone changes occurred in Italy and concerning the bidding zones DE-AT-LU and DE-LU, which were considered as described in the supplementary information. The aggregated net exports were calculated using the total scheduled exchange considering all neighbors. The nuclear availability is obtained by subtracting the unavailable nuclear capacity from the total installed nuclear capacity. Here, we only consider unavailability due to planned maintenance and outages longer than 24 hours, since shorter outages are assumed to not affect the day-ahead price.

In this work, the sum of the European emission trading system (EU ETS) and a carbon tax is referred to as carbon price [39]. The World Group Bank [40] provides EU ETS and carbon tax data in US\$/tCO₂e which was converted to EUR/tCO₂e at a fixed exchange rate of 0.93 EUR/US\$ on 2024-05-07 [41].

Data on the share of natural gas in the electricity mix and the dependency on Russian gas imports are available at Eurostat [12]. The gas price data was obtained from the TTF daily futures [11]. Missing daily gas prices were interpolated. Raw data was converted from US\$ to EUR using the aforementioned exchange rate.

OpenMeteo’s Historical Weather API [42] provides hourly air temperature at 2 m height based on raw data by ERA5 [43]. The mean air temperature is calculated by averaging over points of a grid as described in the supplementary information. The API Hub’Eau [44] provides hourly data of river temperatures and daily data of river flow rates in France. Mean river flow and river temperature were averaged, while only considering rivers near nuclear power plants (see Supplementary Information for details).

The binary variable “Is working day?” of the linear causal models is True for working days. Data on french public holidays was gathered from Ref. [45]. The cyclical variables Day of the year and Hour of Day are parameterized by sinus and cosine functions.

Implementation of SCMs

We use the DoWhy python package [46, 47] to perform the causal analysis. First a causal model is created based on the causal graph shown in Fig. 3. The corresponding graph is implemented with the Networkx python package [48].

Then a structural causal model is created by assigning a causal mechanism to every node. Within the model, root nodes are assumed not to be caused by anything. They are thus assigned an empirical distribution sampled from the normalized data. To non-root nodes a linear regression model with additive noise is assigned, where the noise accounts for unobserved variables. The model is fitted to the normalized data. Model evaluation results are provided in the supplementary information.

The data is normalized by subtracting the mean and dividing by the standard deviation of each variable to ensure numerical stability

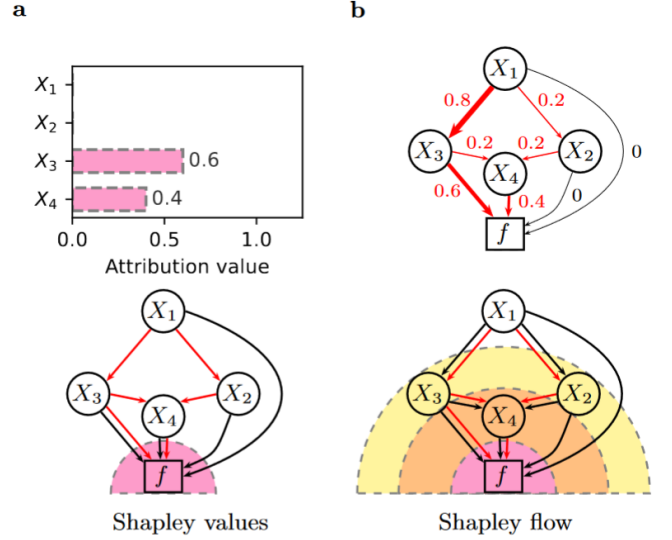


FIG. 8. **Model Explanations via Shapley flows.** The figure illustrates model explanation concepts for an elementary example with four input features $X_{1,2,3,4}$ and no noise. **(a)** Ordinary Shapley values cover only direct influences (edges entering the pink area). When independently perturbing features, X_1 and X_2 have no influence on the target such that their attribution value vanishes. **(b)** Shapley flows consider feature perturbations that are not independent, but are consistent to the data for different explanation boundaries (coloured areas). Hence they can capture both direct and indirect effects. The figure is adapted from [21].

during fitting. The normalized data is thus given by

$$X_{j,norm} = (X_j - \langle X_j \rangle) / \sigma_{X_j}. \quad (3)$$

The structural coefficients resulting from the fitting are then denormalized after fitting. This is achieved by multiplying by the standard deviation

$$c_{ij} = c_{ij,norm} \cdot \frac{\sigma_{X_i}}{\sigma_{X_j}}. \quad (4)$$

GBT models

For the GBT model, we use the XGBoost Python package [49]. In order to find the best hyperparameters for training the gradient boosting trees, we carry out a random search. Further, the model is trained on 80 percent of the data while the remaining 20 percent is used for testing. To prevent overfitting, the time series data is split in the following way into test and train sets: all data points are grouped into four-day intervals, and each interval is randomly assigned to the test or train set according to the 80 percent split percentage. Note that the causal graph is not included in the GBT, hence all features are considered as inputs for the model, without taking into account any dependences of the features in the model. Hence, the concept of causal explanations in the model is introduced only ex-post via Shapley flows.

Shapley flows

Shapley Additive exPlanations (SHAP) [33] are one of the most used explanation tools for machine learning models. They attribute

the outcome of a model to the features respecting the axiomatic properties linearity, efficiency and null player. One limitation is that all features are treated equivalently impeding a causal interpretation. If one perturbs features independently to quantify their impact on the target, then only direct interactions are attributed (Fig. 8a). If one perturbs features according to the initial dataset, then only root nodes are attributed. This is referred to as asymmetric Shapley values.

In contrast, Shapley flows attribute the model outcome to the edges in the causal graph, see (Fig. 8b). A key concept is the boundary of an explanation, which partitions the causal graph into two sets. For Shapley flows, we compute the causal flow along all possible boundaries and thereby edges within the causal graph. Shapley flows retain the axiomatic properties of Shapley values (linearity, efficiency and null player), while introducing a boundary consistency property that states that edge attributions have to be consistent in all their potential boundaries constellations.

Data availability.

Natural gas prices with daily resolution were obtained from Ref. [11] and are subject to copyright. All other data used in this study are publicly available from the respective sources as described in the Methods section.

Code availability.

Computer code is available on github [50].

* These authors contributed equally.

† d.witthaut@fz-juelich.de

- [1] Chalvatzis, K. J. & Ioannidis, A. Energy supply security in the EU: Benchmarking diversity and dependence of primary energy. *Applied Energy* **207**, 465–476 (2017).
- [2] Pedersen, T. T., Gøtske, E. K., Dvorak, A., Andresen, G. B. & Victoria, M. Long-term implications of reduced gas imports on the decarbonization of the european energy system. *Joule* **6**, 1566–1580 (2022).
- [3] Goodell, J. W., Gurdgiev, C., Paltrinieri, A. & Piserà, S. Global energy supply risk: Evidence from the reactions of european natural gas futures to nord stream announcements. *Energy Economics* **125**, 106838 (2023).
- [4] Goldthau, A. & Tagliapietra, S. Energy crisis: five questions that must be answered in 2023. *Nature* **612** (2022).
- [5] Gars, J., Spiro, D. & Wachtmeister, H. The effect of european fuel-tax cuts on the oil income of russia. *Nature Energy* **7**, 989–997 (2022).
- [6] Ruhnau, O., Stiewe, C., Muessel, J. & Hirth, L. Natural gas savings in germany during the 2022 energy crisis. *Nature Energy* **8**, 621–628 (2023).
- [7] European Commission. REPowerEU Plan (COM/2022/230 final). <https://eur-lex.europa.eu/legal-content/EN/TXT/?uri=COM:2022:230:FIN> (2022).
- [8] Council of the EU and the European Council. Where does the EU’s gas come from? <https://www.consilium.europa.eu/en/infographics/where-does-the-eu-s-gas-come-from/> (2025).
- [9] Trebbien, J., Tausendfreund, A., Rydin Gorjão, L. & Witthaut, D. Patterns and correlations in european electricity prices. *Chaos: An Interdisciplinary Journal of Nonlinear Science* **34** (2024).
- [10] European Network of Transmission System Operators for Electricity. Electricity Market Transparency — entsoe.eu. <https://www.entsoe.eu/data/transparency-platform/>. [Accessed 06-02-2025].
- [11] Thomson Reuters Workspace. Tba.
- [12] Eurostat. Eurostat data browser. https://ec.europa.eu/eurostat/databrowser/explore/all/envir?lang=en&subtheme=nrg.nrg_quant.nrg_quanta&display=list&sort=category. [Accessed 06-02-2025].
- [13] Jenkins, J. D., Luke, M. & Thernstrom, S. Getting to zero carbon emissions in the electric power sector. *Joule* **2**, 2498–2510 (2018).
- [14] Haywood, L., Leroutier, M. & Pietzcker, R. Why investing in new nuclear plants is bad for the climate. *Joule* **7**, 1675–1678 (2023).
- [15] Pahle, M. *et al.* Safeguarding the energy transition against political backlash to carbon markets. *Nature Energy* **7**, 290–296 (2022).
- [16] Brown, T. & Reichenberg, L. Decreasing market value of variable renewables can be avoided by policy action. *Energy Economics* **100**, 105354 (2021).
- [17] Khodayar, M., Liu, G., Wang, J. & Khodayar, M. E. Deep learning in power systems research: A review. *CSEE Journal of Power and Energy Systems* **7**, 209–220 (2020).
- [18] Strielkowski, W., Vlasov, A., Selivanov, K., Muraviev, K. & Shakhnov, V. Prospects and challenges of the machine learning and data-driven methods for the predictive analysis of power systems: A review. *Energies* **16**, 4025 (2023).
- [19] Schölkopf, B. *et al.* Toward causal representation learning. *Proceedings of the IEEE* **109**, 612–634 (2021).
- [20] Pearl, J., Glymour, M. & Jewell, N. P. *Causal inference in statistics: A primer* (John Wiley & Sons, 2016).
- [21] Wang, J., Wiens, J. & Lundberg, S. Shapley flow: A graph-based approach to interpreting model predictions. In *International Conference on Artificial Intelligence and Statistics*, 721–729 (2021).
- [22] Banque de France. Energy balance in 2022: the crisis in nuclear power generation came at the worst possible time. <https://www.banque-france.fr/en/publications-and-statistics/publications/energy-balance-2022-crisis-nuclear-power-generation-came-worst-possible-time> (2023). Accessed on 2025-02-07.
- [23] Praktiknjo, A. & Erdmann, G. Renewable electricity and backup capacities: an (un-) resolvable problem? *The Energy Journal* **37**, 89–106 (2016).
- [24] Trebbien, J., Gorjão, L. R., Praktiknjo, A., Schäfer, B. & Witthaut, D. Understanding electricity prices beyond the merit order principle using explainable AI. *Energy and AI* **13**, 100250 (2023).
- [25] European Network of Transmission System Operators for Electricity (ENTSO-E). Single Day-ahead Coupling (SDAC). https://www.entsoe.eu/network_codes/cacm/implementation/sdac/. Accessed on 2024-01-07.
- [26] Van den Bergh, K. & Delarue, E. Cycling of conventional power plants: Technical limits and actual costs. *Energy Conversion and Management* **97**, 70–77 (2015).

- [27] Sensfuß, F., Ragwitz, M. & Genoese, M. The merit-order effect: A detailed analysis of the price effect of renewable electricity generation on spot market prices in germany. *Energy policy* **36**, 3086–3094 (2008).
- [28] ALL NEMO COMMITTEE. Euphemia Public Description. Tech. Rep. (2020). <https://www.nemo-committee.eu/assets/files/euphemia-public-description.pdf>.
- [29] Guénand, Y. *et al.* Climate change impact on nuclear power outages-part i: A methodology to estimate hydro-thermic environmental constraints on power generation. *Energy* **307**, 132648 (2024).
- [30] Van Vliet, M. T. *et al.* Global river discharge and water temperature under climate change. *Global Environmental Change* **23**, 450–464 (2013).
- [31] Van Vliet, M. T., Wiberg, D., Leduc, S. & Riahi, K. Power-generation system vulnerability and adaptation to changes in climate and water resources. *Nature Climate Change* **6**, 375–380 (2016).
- [32] Pechan, A. & Eisenack, K. The impact of heat waves on electricity spot markets. *Energy Economics* **43**, 63–71 (2014).
- [33] Lundberg, S. M. *et al.* From local explanations to global understanding with explainable AI for trees. *Nature machine intelligence* **2**, 56–67 (2020).
- [34] Heinen, S., Mancarella, P., O’dwyer, C. & O’malley, M. Heat electrification: The latest research in europe. *IEEE Power and Energy Magazine* **16**, 69–78 (2018).
- [35] Pfenninger, S. Energy scientists must show their workings. *Nature* **542**, 393–393 (2017).
- [36] Réseau de Transport d’Électricité. French Annual Electricity Review 2022. <https://analysesetdonnees.rte-france.com/en/electricity-review-keyfindings>. [Accessed 14-02-2025].
- [37] European Network of Transmission System Operators for Electricity. Python client for the ENTSO-E API. <https://github.com/EnergieID/entsoe-py>. [Accessed 06-02-2025].
- [38] European Network of Transmission System Operators for Electricity. Single Day-ahead Coupling. https://www.entsoe.eu/network_codes/cacm/implementation/sdac/. [Accessed 06-02-2025].
- [39] Commissariat général au développement durable. Carbon pricing around the world. <https://www.statistiques.developpement-durable.gouv.fr/edition-numerique/chiffres-cles-du-climat-2023/en/17-carbon-pricing-around-the-world>. [Accessed 06-02-2025].
- [40] World Bank Group. State and trends of carbon pricing dashboard. <https://carbonpricingdashboard.worldbank.org/compliance/price>. [Accessed 06-02-2025].
- [41] European Central Bank. Euro foreign exchange reference rates. https://www.ecb.europa.eu/stats/policy_and_exchange_rates/euro_reference_exchange_rates/html/index.en.html. [Accessed 07-05-2024].
- [42] Open Meteo. Free Open-Source Weather API. <https://open-meteo.com/>. [Accessed 06-02-2025].
- [43] Hersbach, H. *et al.* The era5 global reanalysis. *Quarterly Journal of the Royal Meteorological Society* **146**, 1999–2049 (2020).
- [44] Office français de la biodiversité. Eau france: Hub’eau. <https://hubeau.eaufrance.fr/>. [Accessed 06-02-2025].
- [45] République française. Jours fériés en France. <https://www.data.gouv.fr/en/datasets/jours-feries-en-france/>. [Accessed 06-02-2025].
- [46] Sharma, A. & Kiciman, E. Dowhy: An end-to-end library for causal inference. *arXiv preprint arXiv:2011.04216* (2020).
- [47] Blöbaum, P., Götz, P., Budhathoki, K., Mastakouri, A. A. & Janzing, D. Dowhy-gcm: An extension of dowhy for causal inference in graphical causal models. *Journal of Machine Learning Research* **25**, 1–7 (2024).
- [48] Hagberg, A., Swart, P. & Chult, D. Exploring network structure, dynamics, and function using networkx (2008).
- [49] Chen, T. & Guestrin, C. XGBoost: A Scalable Tree Boosting System. In *Proceedings of the 22nd ACM SIGKDD International Conference on Knowledge Discovery and Data Mining*, KDD ’16, 785–794 (Association for Computing Machinery, New York, NY, USA, 2016).
- [50] Tausendfreund, A., Schreyer, S. & Immig, F. Understanding the european energy crisis through structural causal models. <https://github.com/ulrich-oberhofer/Understanding-the-European-energy-crisis-through-structural-causal-models> (2025).
- [51] Trasmissione Elettricità Rete Nazionale. Le nuove zone del mercato elettrico: quello che c’è da sapere. <https://lightbox.terna.it/en/insight/new-electricity-market-zones>. [Accessed 24-01-2024].
- [52] Fast and easy gridding of point data with geopandas — james-brennan.github.io. https://james-brennan.github.io/posts/fast_gridding_geopandas/. [Accessed 13-05-2025].
- [53] Eulig, E., Mastakouri, A. A., Blöbaum, P., Hardt, M. & Janzing, D. Toward falsifying causal graphs using a permutation-based test. In *Proceedings of the AAAI Conference on Artificial Intelligence*, vol. 39, 26778–26786 (2025).
- [54] Draper, N. & Smith, H. *Applied Regression Analysis* (Wiley, New York, NY, 1998), 3rd edn. Includes disk.

Acknowledgements

We thank Max Kleinebrahm and Wolf Fichtner for stimulating discussions.

Author Contributions

D.W. conceived research. D.W. and B.S. designed and supervised research. A.T. and S.S. carried out the initial statistical analysis, implemented and evaluated the linear SCM and designed the respective figures with initial inputs by J.T. F.I. and U.O. implemented the GBT model and evaluated the Shapley flows and designed the respective figures. All authors contributed to discussing the results and writing the manuscript.

Competing Interests

The authors declare no competing financial or non-financial interests.

Additional Information

Supplementary Information is available for this paper.

Correspondence and requests for materials should be addressed to Dirk Witthaut (email: d.witthaut@fz-juelich.de) or Benjamin Schäfer (email: benjamin.schaefer@kit.edu).

SUPPLEMENTARY INFORMATION

DATA SOURCES AND PRE-PROCESSING

Data is obtained and processed as explained in the main text. Here we provide additional information.

Multiple bidding zone changes occurred during the period of investigation. Austria left a shared bidding zone with Germany and Luxembourg in 2018. The time series data of the bidding zone DE-AT-LU (until 2018-09-30) are therefore combined with the one of DE-LU (from 2018-10-01 onwards). The Italian bidding zones were modified on 2019-01-01 and on 2021-01-01 [51]. The production hubs IT-Brindisi, IT-Foggia and IT-Priolo were removed on 2019-01-01. On 2021-01-01, the production hub IT-Rossano was removed and the bidding zone IT-Calabria added. Meanwhile the region Umbria moved from IT-Centre-North to IT-Centre-South. The data for the production hubs before removal and the data of IT-Calabria after its addition is aggregated to the bidding zone of IT-South. The bidding zone IT-North, that is considered in the causal model, was not affected.

The aggregated net exports were calculated using the total scheduled exchange considering all neighbors. That is, we add the exports to all neighboring bidding zones and subtract the imports to all neighboring bidding zones. We note that we use the total total scheduled exchanges instead of the day-ahead scheduled commercial exchange for data quality reasons. In particular, the share of missing data is higher for day-ahead values.

The residual load is calculated by subtracting day-ahead solar and wind generation from the day-ahead load. ROR generation is hereby neglected to avoid mixing day-ahead and actual generation data.

The French ministry of the energy transition [39] lists the European emission trading system (EU ETS) and a carbon tax as instruments that put an explicit price on carbon emissions. In this work, their sum is referred to as carbon price. The World Group Bank [40] provides EU ETS and carbon tax data in US\$/tCO₂e. The raw data is converted to EUR/tCO₂e using the exchange rate of 0.93 EUR/US\$ on 2024-05-07 [41].

The gas price data is obtained from the TTF daily futures [11]. The TTF daily futures provide daily values. Missing daily gas prices are interpolated.

The mean air temperature is calculated by dividing France into a grid with code from [52] as displayed in Fig. 9. Open Historical Weather API [42] provides hourly air temperature at 2 m height for each grid point. The mean air temperature is then calculated by averaging.

The API Hub'Eau [44] provides hourly river temperature data and daily river flow rate data. We consider rivers with the highest mean flow rates and those near nuclear power plants: Rhine, Rhône, Loire, Garonne, Seine, Dordogne, Vienne, Moselle, and Meuse. For each river,

we averaged the data from different measuring stations. Then, we averaged both variables over all nine rivers.

All time series used in the analysis are denoted in co-ordinated universal time (UTC) and have an hourly resolution. Some time series, as for example the gas price, are available only with daily resolution. In this case we padded the daily value for all hours of the day.

EVALUATION OF SCMS

DoWhy [46, 47] checks how many local Markov conditions (LMC) are violated in a given graph using conditional independence (CI) tests. During CI tests, the conditional independence of all non-descendants of each node given its parents is checked [53].

Using LMCs wrong graphs can be rejected, but a graph can not be declared as true with certainty. A benchmark is required of how many LMC violations are acceptable, above which graphs are rejected. To get a benchmark, we randomly permute the nodes of a given graph and test for violations of LMCs. The p-value, denoted as p_{LMC} , is defined as the probability of a randomly permuted graph to have fewer LMC violations than the original graph. We accept a given graph if the p-value falls below some threshold; otherwise it is rejected. Graphs of the same Markov equivalence class (MEC) have the same conditional independencies [20]. Thus, if too many of the permuted graphs lie in the same MEC, the conditional independence tests are not informative of the graph's correctness. A second p-value p_{MEC} is defined as the probability of a randomly permuted graph to lie in the same MEC as the given graph. The graph is considered falsifiable if the p-value is below a certain threshold. We use a significance level of 0.05 for both p-values. In conclusion, we say a graph is falsifiable if no more than 5 % of the randomly permuted graphs lie in the same MEC as the given graph. We say a graph is falsified if more than 5 % of the randomly permuted graphs have as few or fewer LMC violations as the given graph.

For both models (electricity price and net exports), the p-value p_{MEC} is zero for 50 random node permuted graphs. None of the randomly permuted graphs lie in the same MEC as the given graphs. Therefore, we conclude that the corresponding causal graphs are falsifiable. To falsify the models, the violation of LMCs are compared against 50 random node permuted graphs. Out of the 236 possible LMC violations, both models – one with electricity prices as the target and the other with net exports – violate 172.. Nevertheless, the p-value p_{LMC} is zero for both models. Therefore, none of the permuted graphs violate as few or fewer LMCs than the original graph. The causal graph thus performs significantly better than random and we accept it.

We use the R² score to evaluate goodness of the fit for

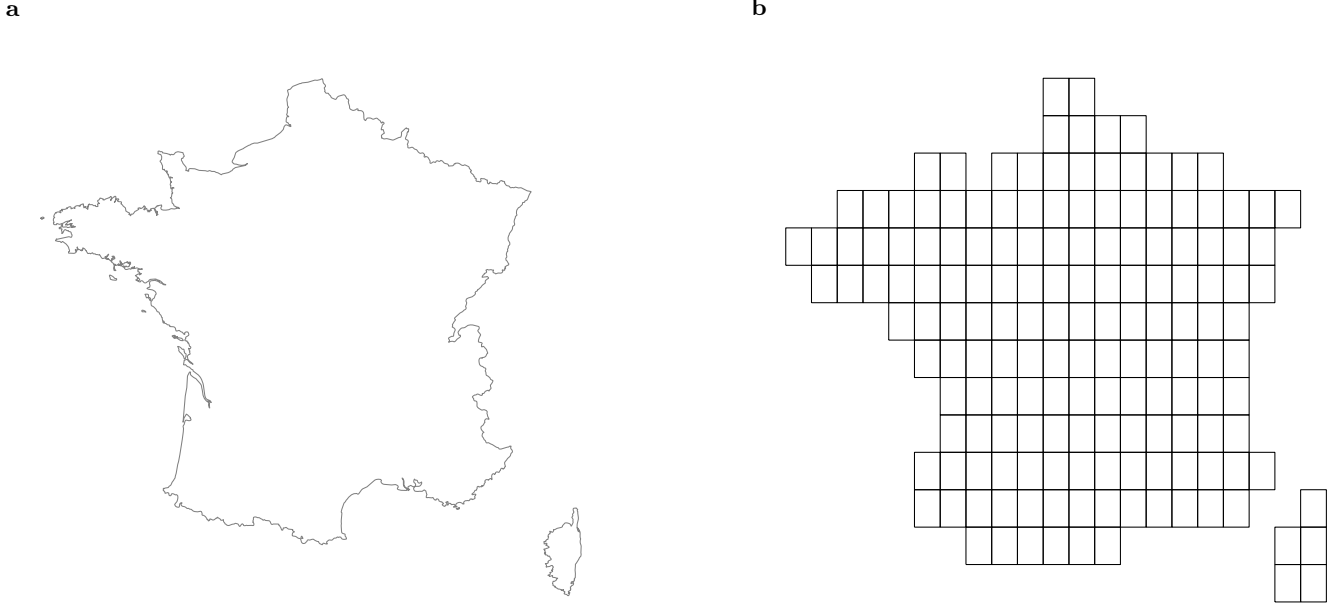


FIG. 9. **Definition of the mean air temperature.** The map of France (a) is split into a grid (b). The air temperature is averaged over all grid points obtain the mean air temperature. Code used is from [52].

every structural equation. The R2 score is defined as

$$R^2 = 1 - \frac{RSS}{TSS}. \quad (5)$$

Hereby, the total sum of squares TSS is the squared difference between observed values and their mean. The residual sum of squares RSS is the squared difference between model prediction and observed values. The ratio of RSS and TSS thus yields the fraction of variance that is not explained by the model. The R2 score thus is the proportion of variance that the model can explain [54].

Different effects can lead to low R2 scores. The used linear model might not be appropriate in case of strongly nonlinear causal effects. Further, relevant variables might be missing which are collectively represented in the noise term (see equation 1). This can lead to the noise term dominating in the structural equation. This mechanism is especially prevalent in highly complex systems featuring many variables and dependencies which can not all be considered in the model. As the electricity market is such a highly complex system, we need to decide which dependencies the model should include and for which variables we accept that they are mostly influenced by noise terms.

The R2 scores of all fits are depicted in Fig. 10. As our analysis focuses on the final targets, the electricity price and the net exports, their corresponding results are most important. We find a R2 score of 0.89 for the electricity price and 0.86 for net exports. Hence, the proportion of variation in the target variables that the model can explain is high. The choice of a linear model, as well as the causal graph, appear to be a reasonable approximation.

All variables relevant to assess model evaluation, the R2 scores of the targets as well as the LMC violations, are listed in Tab. I. The R2 score of the nuclear availability is with 0.44 significantly lower than the R2 scores of the target variables. This is to be expected since many influences onto it are not part of the model. For example, unforeseen corrosion damage lead to many reactors going into revision in 2021 and 2022 [36]. These variables are not included in the model.

Period	R ²	LMC Violations
Target: Price day-ahead		
2018-01-01 – 2023-12-31	0.89	172/236
Target: Net exports		
2018-01-01 – 2023-12-31	0.86	172/236

TABLE I. Model Performance of SCM's for both electricity price and net exports as target.

INDIRECT CAUSAL EFFECTS – HYDROPOWER AND COOLING WATER

In our SCM, the river flow variable enters the models of nuclear availability and run-of-river hydropower, both of which affect the electricity price and the exports. Here we discuss this indirect effect for the net exports, while the indirect effect on the electricity price is discussed in the main text.

In a linear SCM, the indirect causal effect is obtained by simply multiplying the structural coefficients [20]. Summarizing both causal paths, we find that an increase

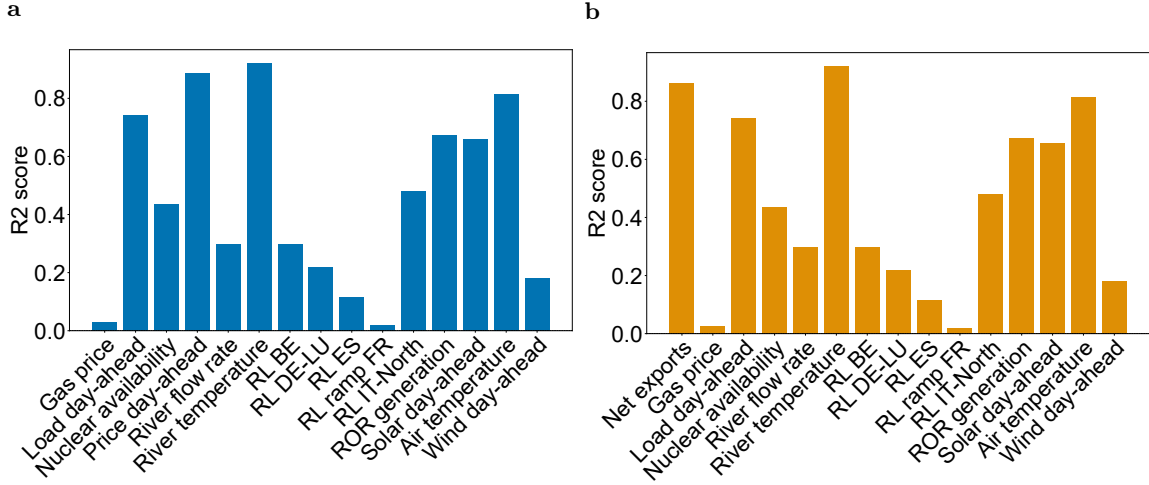


FIG. 10. **R2 scores of non-root nodes of SCMs.** **a**, R2 scores of SCM with electricity price as target. The R2 score of 0.89 of the electricity price indicates the suitability of the causal graph as well as the choice of a linear model. **b**, R2 scores of SCM with net exports as target. The R2 score of 0.86 of the net exports indicates the suitability of the causal graph as well as the choice of a linear model.

in flow of $1 \text{ m}^3/\text{s}$ increases net exports by 7.9 MW on average (Fig. 11). Interestingly, both causal pathways contribute to a similar extent.

SEASONALITY OF NUCLEAR AVAILABILITY, LOAD AND ENERGY PRICES

Essential variables in the French electricity system display a strong seasonality as shown in Fig. 12. The demand for electricity is usually higher in the winter due to the prevalence of electric heaters [34]. Electricity prices are determined by the balance of supply and demand, such that the price generally increases with the demand. In fact, we observe that prices are usually higher in winter than in summer.

The French electricity market heavily relies on nuclear power plants that require revisions. The demand and price are typically lowest during the summer and so are opportunity costs for the unavailability of nuclear power plants. Indeed we observe a pronounced seasonality of nuclear availability which closely follows the seasonality of the load (Fig. 12).

Seasonal affects can induce confounding. Typically, both the nuclear availability and the electricity price are highest in winter as argued above. This can lead to a perceived violation of economic laws if one only considers the supply side and neglects the seasonal variation in demand.

PRICE DIFFERENCES BETWEEN FRANCE AND ITS NEIGHBORS

We use SCMs shown to analyze why French electricity prices strongly increased during the energy crisis even though France does not rely on gas. We conclude that two factors caused the sharp rise in French electricity prices: The unavailability of French nuclear power plants leads to France being more dependent on its neighbors. This leads to higher French electricity prices during the energy crisis when compared with its neighbors [22].

We analyze the difference of electricity prices in France with respect to the neighboring bidding zones in Fig. 13. Before the energy crisis, price differences with respect to Spain (ES), Belgium (BE) and Germany-Luxembourg (DE-LU) are generally small. They are mostly negative for ES and vary between positive and negative values for BE and DE-LU. During the crisis, price differences with respect to these neighbors increase sharply. Positive values are much more frequent than negative values, indicating imports from the respective bidding zones to France. Hence, the French electricity market could not decouple from its neighbors, which have a substantial share of natural gas in the electricity mix.

The situation is different for the bidding zone IT-North. Italy frequently imports electric power from its neighbors [9] and often sees comparably high electricity market prices. Accordingly, price differences between France and IT-North are often negative. During the energy crisis, the monthly average of the price difference remained negative while the standard deviation increased strongly.

Overall, the correlations of electricity prices with Italy increased during the energy crisis [9] contrary to the other

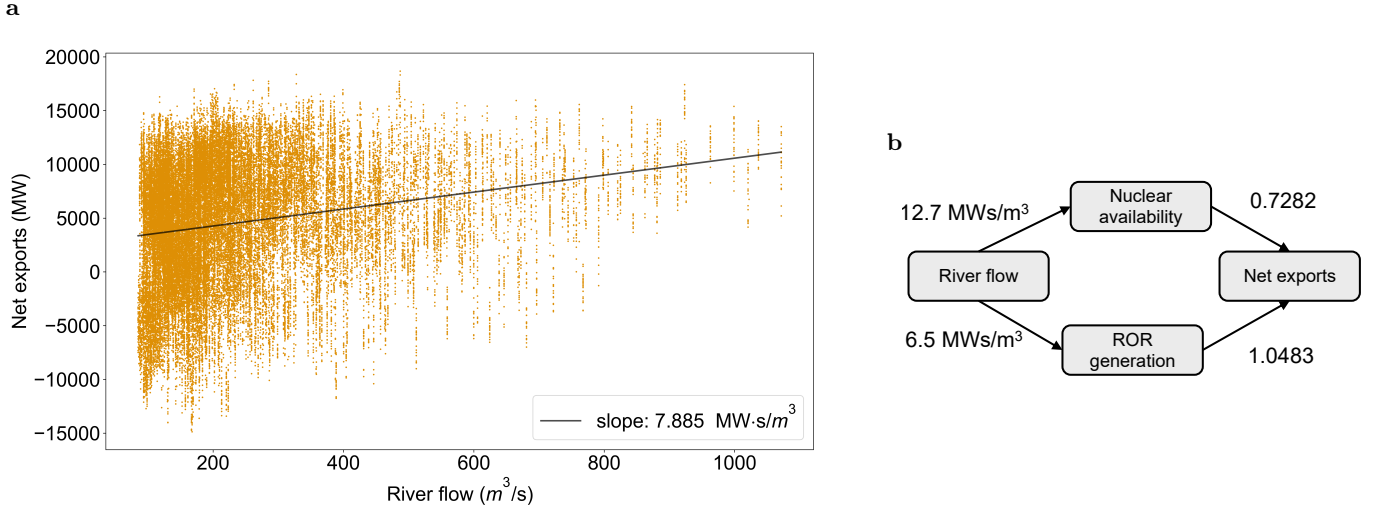


FIG. 11. **Indirect impact of river flow on net exports.** **a**, Scatter plot of the net exports against the river flow rate. A linear regression yields a slope of $7.9 \text{ MW} \cdot s/m^3$. **b**, Extract of the causal graph showing the indirect impact of river flow on net exports through nuclear availability and ROR hydro generation. The arrows indicating causal relations are labeled with the respective structural coefficients. The indirect causal effect is calculated by multiplying the structural coefficients of each causal path and summarizing both paths. This leads to an indirect causal effect $16.1 \text{ MW} \cdot s/m^3$, significantly more than the regression coefficient. The discrepancy can be explained by confounding due to seasonality effects.

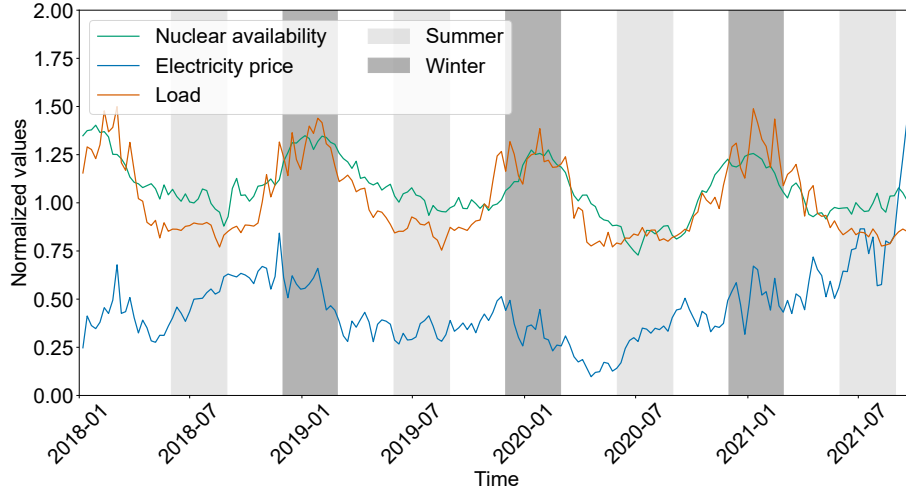


FIG. 12. **Seasonality in the French electricity system.** We plot the weekly averages of the nuclear availability, load, and the day-ahead electricity price before the start of the energy crisis normalized by their respective overall means. Winter and Summer are indicated with gray areas. Nuclear availability is highest in the winter, which can be explained by revisions being scheduled in summer when load is lowest. Electricity prices are higher in case of higher load, causing positive correlation between nuclear availability and electricity prices.

neighbors. That is, electricity prices in France showed similar patterns it Italy, where natural gas provides contributes substantially to electricity generation (see main text).

PERFORMANCE OF GBT MODELS

We complement the usage of SCM with GBTs, as these can model non-linearities in the data. Hence, we also observe a better performance of the GBT models compared to the SCM models, see Table II compared to Fig. 10. While the difference between 0.8 and 0.9 might not seem large at first glance, this reduces the unexplained variance from 20% to 10%.

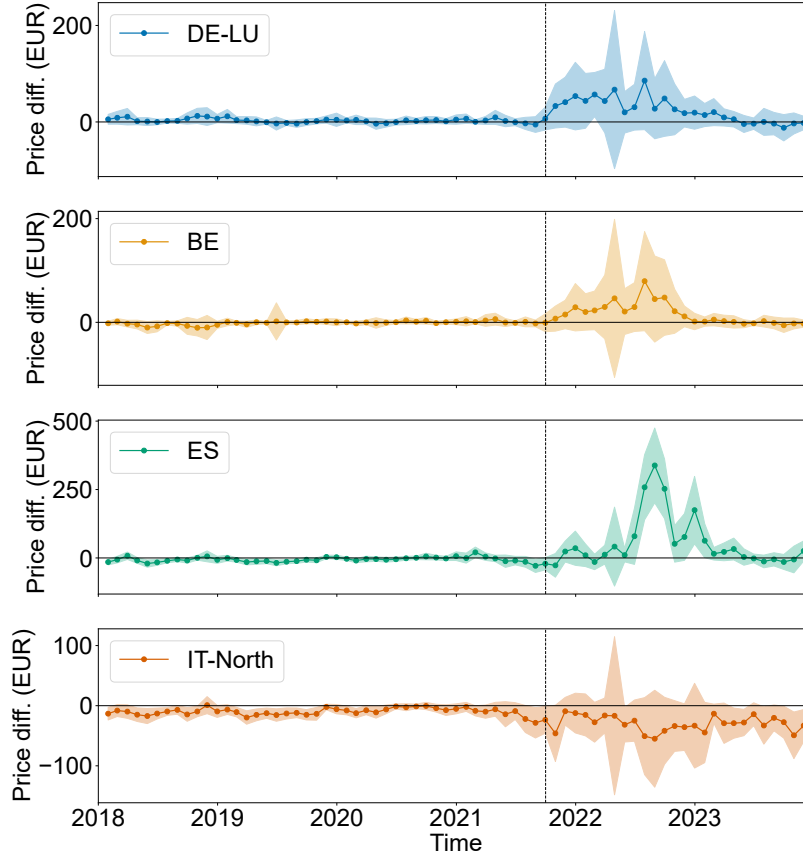


FIG. 13. **Differences of French electricity prices with respect to the neighboring bidding zones.** We provide a monthly aggregated statistics, where the circles give the mean and the shaded area indicates the standard deviation. The solid line is drawn to guide the eye. The beginning of the energy crisis defined as 1st October 2021 is marked with a dotted line.

Period	R^2	MAE	RMSE	Mean Label
Target: Price day-ahead				
2018-01-01 – 2021-09-30	0.92	5.17	9.25	53.52
2021-10-01 – 2023-12-31	0.82	21.82	63.39	184.90
2018-01-01 – 2023-12-31	0.96	12.41	22.90	107.04
Target: Net exports				
2018-01-01 – 2021-09-30	0.86	1318.04	1707.30	5907.20
2021-10-01 – 2023-12-31	0.92	1397.22	1781.68	1741.07
2018-01-01 – 2023-12-31	0.91	1291.24	1639.17	4172.89

TABLE II. GBT performance metrics over the different time periods and for both, prices and exports from France.

FURTHER SHAPLEY FLOW RESULTS

Here we provide additional results for Shapley flows in the GBT model. This analysis complements the results of the model of the net exports in the main text.

An overview of the Shapley flows in the model of the electricity price is provided in Fig. 14. As in the linear SCM, the gas price is the most important feature, complemented by the carbon price and the nuclear availability. The most pronounced indirect effects are via river

flow rate on ROR generation on the electricity price.

Furthermore, we show dependency plots in Fig. 15, analogous to the main text. Again, we observe a constant effect of the air temperature via the load on the target for temperatures above 10°C (panel a). The correlation between temperature and Shapley flow is negative for low temperatures as low temperatures increase the load and thereby increase the prices. Similar effects are observed on the indirect river flow rates as for the net exports (panels c, e). Contrary to the model for the net exports, the direct influence of the features (panels b, d, f) is also non-linear.

Finally, we also display SHAP dependency plots for the net export target in Fig. 16. While the load and nuclear availability features (panels a and b) are again linear, consistent with the Shapley flows from the main text, the effects of river flow and temperature (panels c and d) are more complex and harder to interpret than the disentangled Shapley flows. The river flow feature is very scattered, making it hard to interpret. Meanwhile the temperature dependency is non-monotonous, likely because the temperature has positive correlations

via some features (e.g. the load day-ahead as shown in the main text) and negative correlations via others. This

result furthermore emphasizes the usefulness of Shapley flows in the analysis of machine learning models with a complex causal structure.

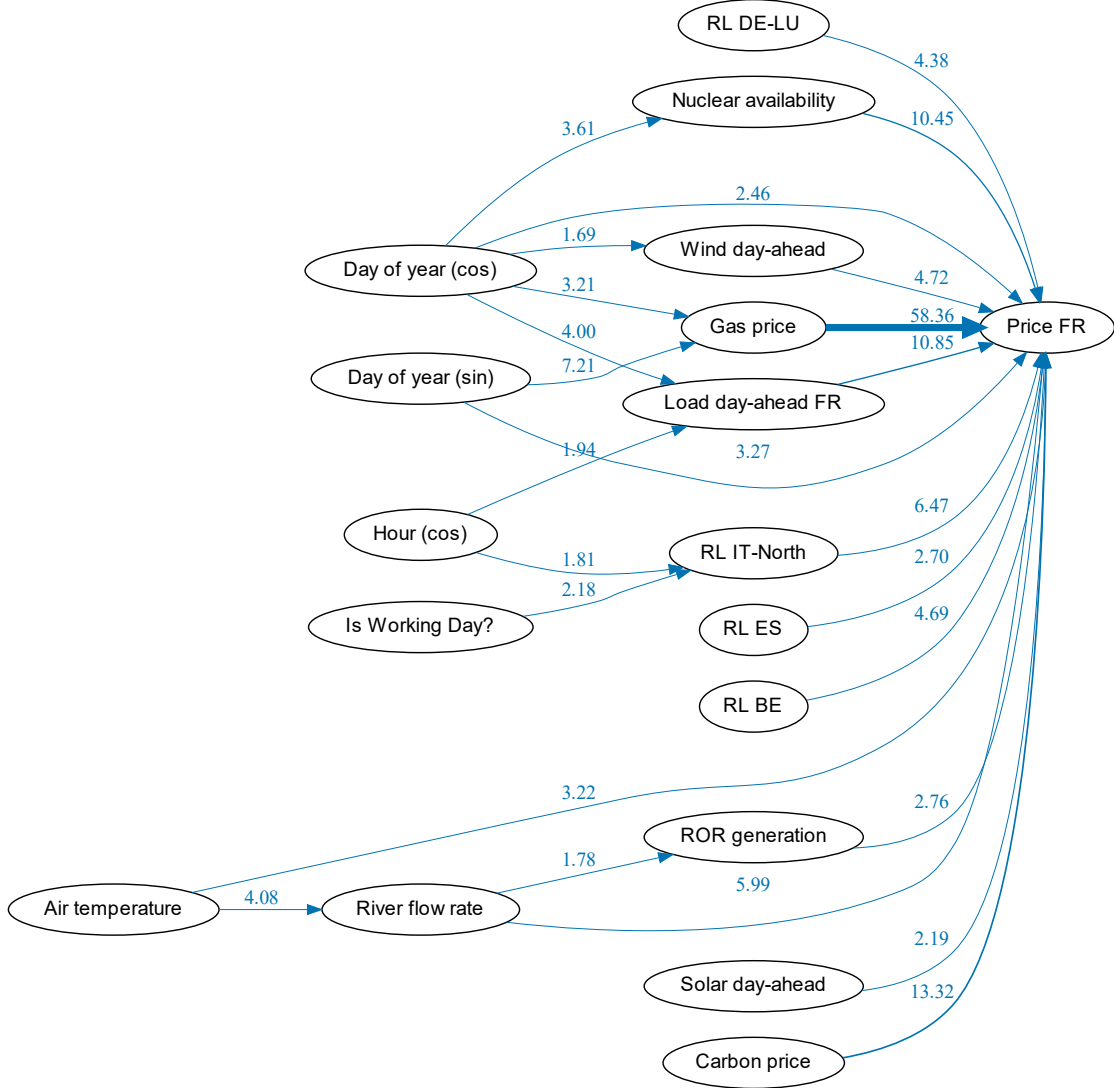


FIG. 14. **Shapley flows explain the non-linear GBT model for the day-ahead prices.** All feature and the target node of the causal graph are shown. In contrast to the causal graph shown in in the main text, only the 25 most important edges are shown. The edge attributions quantify how a given feature directly or indirectly influences the target prediction. For example, the Air temperature feature has both relevant direct and indirect effects across the graph.

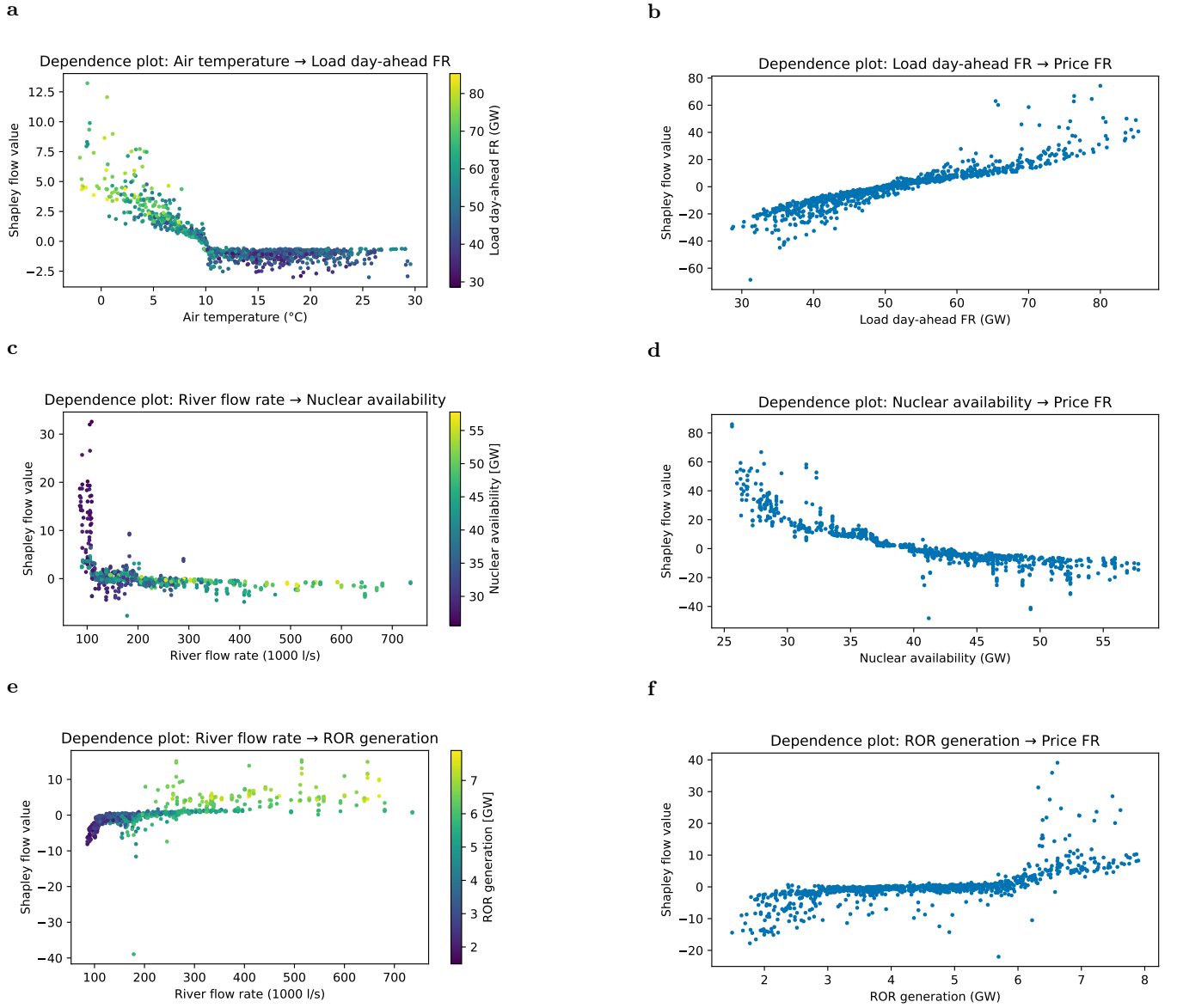


FIG. 15. Shapley flow analysis reveal direct linear and indirect non-linear dependencies. We display Shapley flow dependencies plots for the target of electricity prices. We follow the causal flow from Air temperature via day-ahead load (a) to the target (b). Similarly, we visualize how river flow rate impacts nuclear availability (c), which in turn affects prices (d) or how the river flow rate influences exports via the ROR (e) or ROR directly impacts prices (f).

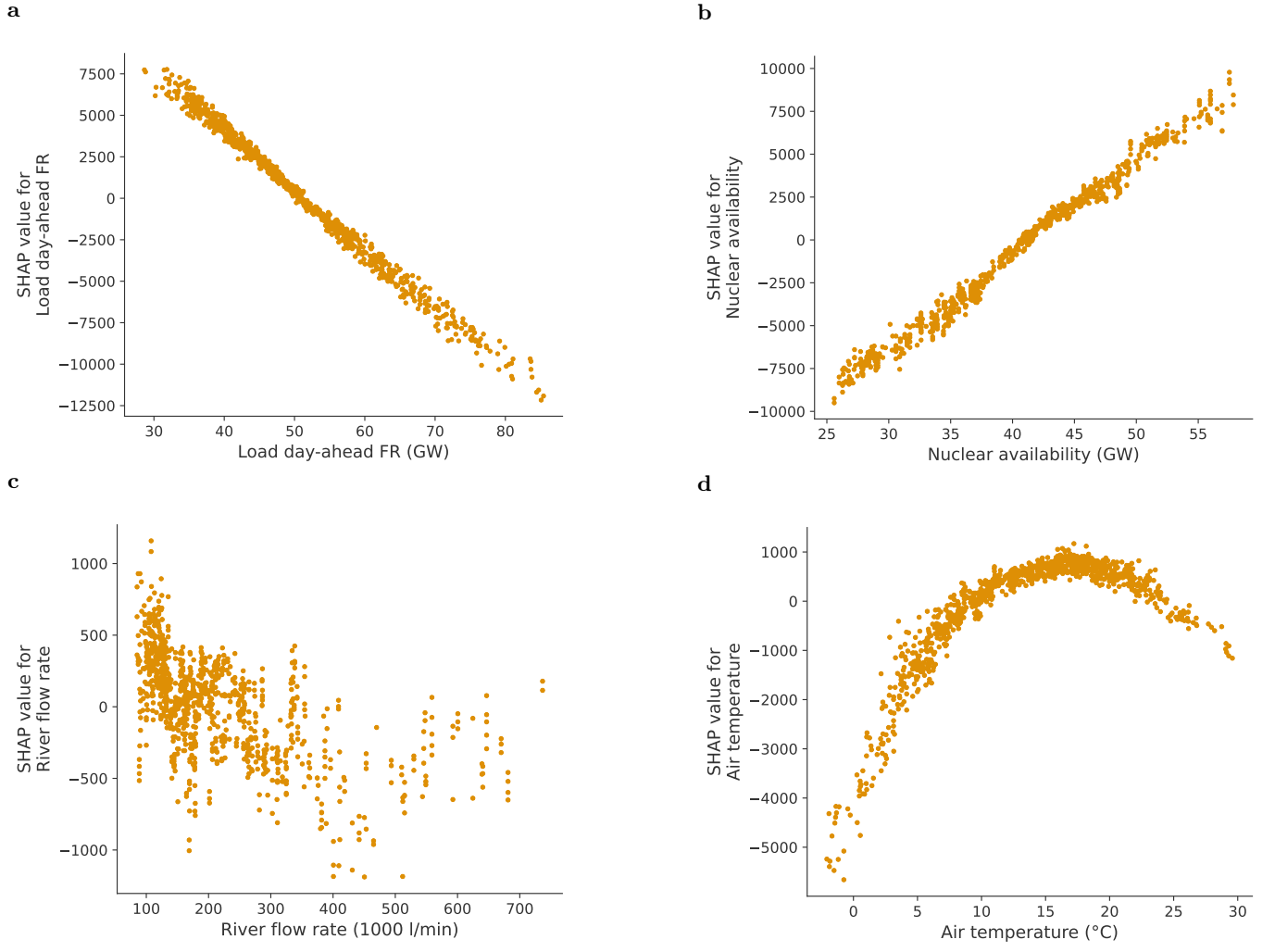


FIG. 16. **SHAP dependence plots miss indirect effects.** We display SHAP dependencies plots for the target of net export. No flows or indirect effects can be disentangled with SHAP values.